

Development of the ITER Advanced Steady State and Hybrid Scenarios

C. E. Kessel 1), A. H. Kritz 2), T. Rafiq 2), G. Bateman 2), D. C. McCune 1), R. V. Budny 1), D. Campbell 3), T. Casper 3), Y. Gribov 3), and J. Snipes 3)

1) Princeton Plasma Physics Laboratory, P.O. Box 451, Princeton, NJ, USA

2) Lehigh University, Lehigh, PA, USA

3) ITER Organization, Route de Vinon sur Verdon, 13115 Saint Paul Lez Durance, France

email: ckessel@pppl.gov

Abstract. Full discharge simulations are performed to examine the plasma current rampup, flattop and rampdown phases self-consistently with the poloidal field (PF) coils and their limitations, plasma transport evolution, and heating/current drive (H/CD) sources. Steady state scenarios are found that obtain 100% non-inductive current with $I_p = 7.3\text{-}10.0$ MA, $\beta_N \sim 2.5$ for $H_{98} = 1.6$, Q 's range from 3 to 6, $n/n_{Gr} = 0.75\text{-}1.0$, and NB, IC, EC, and LH source have been examined. The scenarios remain within CS/PF coil limits by advancing the pre-magnetization by 40 Wb. Hybrid scenarios have been identified with 35-40% non-inductive current for $I_p = 12.5$ MA, $H_{98} \sim 1.25$, with $q(0)$ reaching 1 at or after the end of rampup. The equilibrium operating space for the hybrid shows a large range of scenarios can be accommodated, and access 925-1300 s flattop burn durations.

1. Introduction

ITER[1] will provide critical information on advanced burning plasma scenarios of interest for fusion power plants by pursuing hybrid and steady state discharges. These scenarios operate at lower plasma current and higher β_N than the baseline ELMy H-mode inductive scenario, and will have longer flattop burn phases of 1000 and 3000 s, respectively. The fusion gain is expected to be approximately 7 and 5, with ~30-50% and 100% of the plasma current being driven non-inductively (including bootstrap current) for the hybrid and steady state scenarios. They will have different current profiles, the hybrid will have a minimum safety factor near 1.0 with a broad flat shear region, while the steady state plasmas will have safety factor values greater than 1.5-2.0 with a profile determined by the heating and current drive (H/CD) sources and bootstrap current. Full discharge simulations are performed to examine the plasma current rampup, flattop and rampdown phases self-consistently with the poloidal field (PF) coils and their limitations, plasma transport evolution, and heating/current drive (H/CD) sources. These time dependent self-consistent free-boundary calculations are performed with the Tokamak Simulation Code (TSC)[2] and PTRANSP[3] transport evolution codes coupled together. A steady state discharge scenario is shown in Fig. 1, for the plasma current contributions, I_i , β values, elongation, and flux state.

2. Hybrid and Steady State Scenarios

The hybrid scenario is targeting plasma current values of ~12.5 MA, with a full size plasma ($R=6.2$ m, $a=2.0$ m, $\kappa=1.85$). The H/CD sources are ion cyclotron (IC) and neutral beams (NB), with possible inclusion of electron cyclotron (EC). The transport regime is an H-mode with some enhanced energy confinement over the IPB98(y,2) scaling, and is subsequently modeled with flat density profiles and approximate H_{98} multipliers of 1.25 derived from simulations with GLF23[4] and MMM08[5] theory based transport models. The pedestal pressure is determined from EPED1[6] analysis

for the hybrid, giving a pedestal temperature of about 3.9-4.5 keV at the location of $\rho_{\text{ped}} \sim 0.94$, and at a central density of $0.85 \times 10^{20} / \text{m}^3$ ($0.6 \times 10^{20} / \text{m}^3$ at the pedestal).

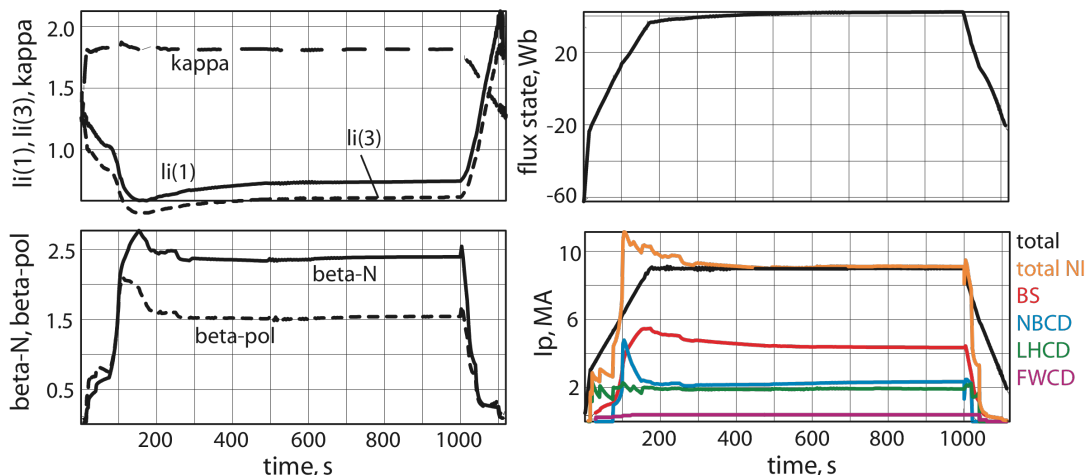


Figure 1. Time histories of the plasma current contributions, normalized and poloidal beta, flux state, li and elongation for a steady state discharge simulation utilizing NB, LH, and IC. The simulation is run to 1000s and then rampdown is initiated.

The steady state scenario is targeting plasma current values of 7-10 MA, with a full size plasma, such as shown in Fig. 2. The H/CD sources are IC, NB, EC, and lower hybrid (LH). The transport regime is very difficult to prescribe for this scenario and so is modeled with 3 approaches. Beginning with the pedestal prediction from EPED1 analysis, giving a pedestal temperature of about 3.3-3.7 keV at the location of $\rho_{\text{ped}} \sim 0.94$, and at a central density $0.65\text{-}0.75 \times 10^{20} / \text{m}^3$ ($0.5\text{-}0.67 \times 10^{20} / \text{m}^3$ at the pedestal), it is found that the core plasma must have enhanced confinement to succeed in reaching 100% non-inductive plasma current and fusion gains (Q) in the range of 3-6. This implies an internal transport barrier (ITB) is required, and so a thermal diffusivity is used that produces such an ITB in the temperature profiles. A target global energy confinement multiplier of $H_{98} \sim 1.6$ is used. Higher values will increase both the non-inductively driven current and the Q. For all cases the density profile is prescribed to have $n(0)/\langle n \rangle$ of 1.0, 1.3, or 1.5. The fuel ions and impurities are given the same density profile shape as the electrons, but their magnitudes are derived from particle balance and prescribed, respectively. The helium concentration is calculated self-consistently. These profiles are shown in Fig. 2. The second approach for the core transport is to use a bifurcation model with suppression of the thermal diffusivity to neoclassical levels wherever the q profile has negative magnetic shear. The third approach is to use theory based models, with no adjustable parameters, to search for conditions where enhanced core transport can be obtained, and is reported in detail in ref[3]. Results reported here will use the prescribed thermal diffusivity approach.

The plasma configurations must be consistent with the power removal and particle pumping in the divertor. Although scrape-off layer plasma and neutral particle analysis are not done as part of these time-dependent calculations, all scenarios are attempting to elevate the power radiated from the plasma in order to keep the power conducted to the divertor in the proper range[7]. The impurity assumptions are 2% beryllium and 0.4% argon, which provides for 25-45 MW of radiated power, depending on the scenario, and brings the conducted power to the divertor to about 80-100 MW, the appropriate range for the desired heat flux limitations.

For all scenarios the IC is modeled with the TORIC[8] full wave module, NB and alpha particles with the NUBEAM[9] Monte Carlo method, EC with the TORAY[10] ray-tracing module, and LH with the LSC[11] ray tracing 1D Fokker Planck method. From comparisons between LSC and GENRAY/CQL3D[12], a 2D Fokker Planck treatment, on ITER scenarios, a factor of 1.6 in the total driven current has been identified as the discrepancy, and is used here to compensate the result of LSC.

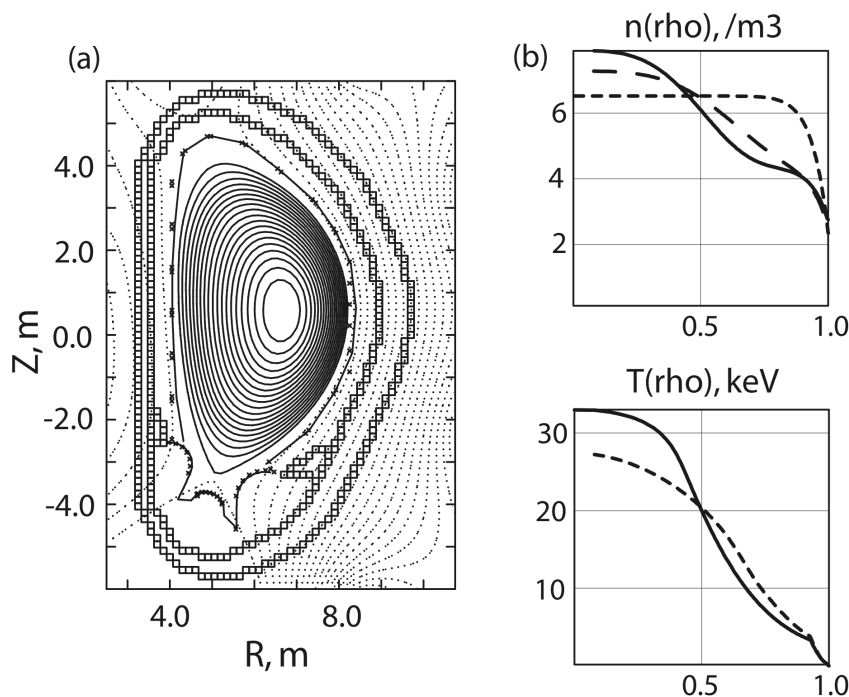


Figure 2. (a) Plasma poloidal flux contours within the vacuum vessel, and first wall and limiter contour for a steady state scenario. (b) Profiles of the plasma density, showing the $n(0)/\langle n \rangle = 1.5$ (peaked), 1.3 (medium), and 1.0 (broad) which are assumed in the simulations. Two profiles of the temperature, which are produced by prescribing the thermal diffusivity profile and its magnitude.

All simulations begin with a large bore 500 kA plasma, as described for the baseline scenario[13]. The plasma is grown to full size and shape by ~ 15 s, when the plasma diverts, and soon after heating begins. The current ramp-up times are varied for the hybrid scenario from 60 to 150 s, while those for the steady state scenario are always 150 s. The primary goal of the hybrid ramp-up is to reach $q(0) \geq 1.0$ at the end of the ramp, avoiding the onset of sawteeth. This requires about 165-175 V-s, and can be accomplished with 2.5-15 MW of heating during the ramp, and with an H-mode onset 2/3 of the way through the ramp or at the end of the ramp. The steady state cases all use a 150 s current ramp-up to avoid injecting excessive inductive current into the plasma. The H/CD begins just after the divert time with significant power levels ramping up to drive non-inductive current approaching the total plasma current. The IC, LH and EC sources are used in the earliest phase of the current ramp-up and continue through the discharge, while the NB are used only after the density permissible is reached (approximately half way through the ramp-up). PTRANSP analysis found that about 3-4 MW of NB power can shine through when the NB's are first turned on at the permissible density, however this can be easily mitigated by delaying the injection. It is found that overdriving the plasma current in the rampup

phase of the steady state scenario has the negative result of causing the central safety factor to rise to high values before dropping to its steady state value, over about 200-400 s. The negative loop voltage provided by the central solenoid (CS) and poloidal field (PF) coils is driven at the plasma edge, and diffuses into the core over the long current diffusion time-scale, resulting in a suppression of current density and elevation of $q(0)$. It can be avoided by keeping the total non-inductive current below the total plasma current until flattop is reached, although the balance of enough power to drive current and to enter the H-mode requires some optimization.

3. Central Solenoid and Poloidal Field Coils

The CS and PF coils must operate within their allowable limits on current, field, and forces. The hybrid scenario is still an inductive discharge, with at least half its plasma current supplied inductively in the flattop. Since the plasma current is lower and the non-inductive current component is higher, the flattop time can be extended. Since fewer V-s are required to rampup the lower plasma current, the current/field in PF6 (divertor coil) can easily be exceeded. This can be relieved by advancing the pre-magnetization state from the maximum of 120 to 90 Wb. The advance is determined by trying to avoid the PF6 current/field limit that is reached at the low end and the reduction in flattop time set by the CS1 coil's current/field limit at the high end. It is found that up to ~ 1300 s flattop times can be reached.

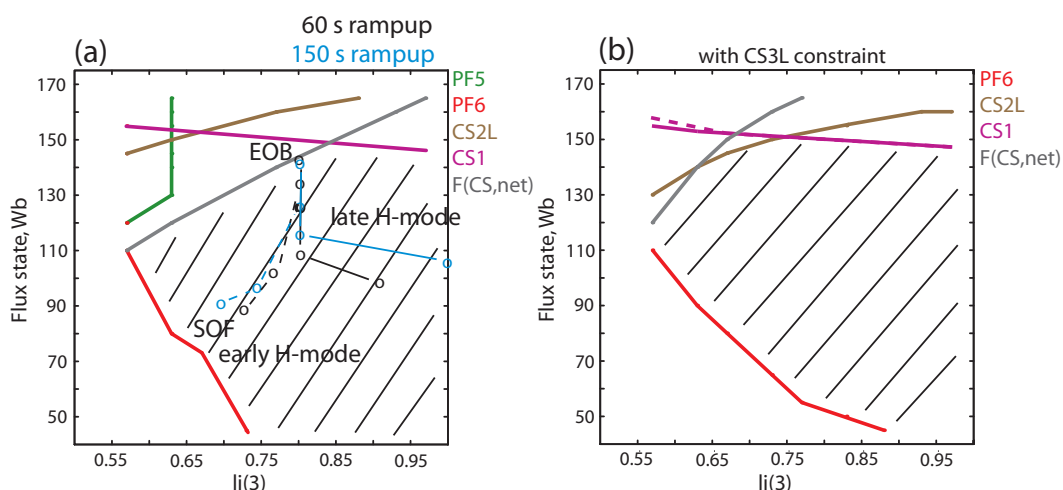


Figure 3. Equilibrium operating space diagrams for the hybrid scenario for $I_p = 12.5$ MA. The left plot (a) shows the operating space is limited by PF6, CS1 and the CS net force, while the right plot (b) shows that a constraint on CS3L can largely remove the CS net force limit. Also shown are trajectories in the operating space for 4 separate hybrid flattop phases from TSC simulations.

The equilibrium operating space is examined as a function of flux state and plasma internal self-inductance[11], at a plasma current of 12.5 MA, and is shown in Fig. 3. The various coils that limit the operating space are shown. Here the nominal plasma boundary points are enforced to have small errors, and show a large operating space available, limited by PF6 at the lower left corner, CS1 at the top, and a combination of PF5 and CS2L at the upper left corner. In addition to these, it is found that the vertical net force on the CS coil stack can give rise to a limit in the operating space. This arises because the advancing of the flux state causes the CS3L coil's current to become negative, which eliminates any vertical separating force, but can lead to an excessive vertical net force as the flux state increases and li decreases. This can be

relieved by forcing the CS3L coil's current to remain positive, and is similar to the current control utilized for the baseline scenario to avoid excessive vertical separating forces[11]. Also shown in Fig. 3 are time dependent simulation trajectories in the operating space from start of flattop (SOF) to end of burn (EOB), either with an early transition to the H-mode 2/3 of the way along the rampup or at the end of the rampup, for a 60 s and 150 s rampup time. These 4 cases reach flattop times of 925-1300 s. Shown in Fig. 4 are the CS/PF coil currents for the 60 s ramp case which reaches 925 s of flattop burn.

The steady state scenario consumes about 85-100 Wb to rampup the plasma current to 7.5-10 MA, with external heating and current drive assisting. Just as in the hybrid case, the low flux consumption can cause the PF6 coil to reach its current/field limit. A 40 Wb advanced pre-magnetization is used to avoid this. In addition, since the plasma current is 100% non-inductive in the flattop the CS and PF coil currents become steady in flattop and so we do not reach any coil limits. The desired flattop phase is about 3000 s. The pre-magnetization could be further optimized for coil currents, field or forces in the flattop. The possible lower I_i values in the steady state scenarios can drive PF6 to large currents, in spite of having low plasma currents. This is illustrated in Fig. 4, with the time history of PF6 coil current for 3 cases with different I_i and I_p values. Although the 40 Wb advanced pre-magnetization is working, the low $I_i(3) = 0.46$ and $I_p = 7.25$ MA case gets close to the coil limit, while the $I_i(3) = 0.7$ and $I_p = 10$ MA case is far from the coils limits.

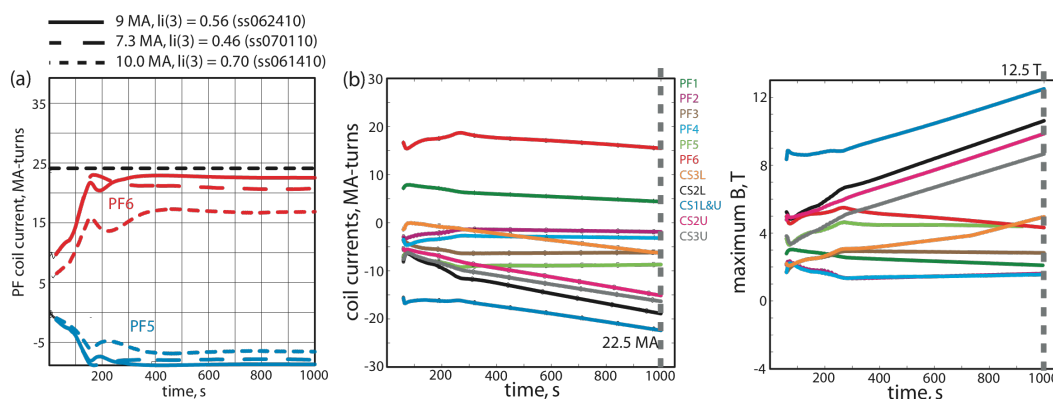


Figure 4. (a) Time histories of the PF6 and PF5 coils for 3 separate steady state scenarios with varying I_p and I_i , showing that low I_i values can drive the PF6 coil current near its limit in spite of a low I_p , and that high I_p does not imply high PF6 current so long as I_i is sufficiently high. (b) CS and PF coil currents in a 60 s rampup hybrid discharge with a late H-mode, showing the CS1 coil approaching its current and field limit by 1000 s, providing about 925 s of flattop burn.

4. Heating and Current Drive Sources

The hybrid scenario has been simulated with NB, steered full off-axis and IC at 53.5 MHz H/CD sources. The NB drives 1.2 MA and the bootstrap current is 3 MA, the remainder is inductive current. The safety factor drops below 1 and a sawtooth model is applied. The resistive phenomena associated with sawtooth avoidance in the presence of 4/3 or 3/2 islands seen in present hybrid experiments is not available in these simulations.

The SS scenario is significantly dependent on the H/CD sources, since the current deposition profiles in combination with the bootstrap current determine the safety factor profile. The powers in each source considered are 33 MW of NB, 20 MW of IC, 20-40 MW of EC, and 20-40 MW of LH. Each of the sources have defined parameters such as frequency, particle energy, spectra, and steering. The NB has 1 MeV particle energy, with the capability to steer from on-axis to off-axis, with a resulting deposition that peaks on-axis or at a ρ of 0.3-0.35. The full off-axis steering is chosen for the SS scenarios, giving about 3 MA of driven current. The ICRF was examined in the frequency range of 48-53.5 MHz to obtain on-axis deposition and accommodate the strong magnetic axis shift, with 48 MHz being chosen for the SS scenarios. A FWCD component is taken to be ~ 200 -400 kA on axis, based on previous ray-tracing analysis[14]. The EC examined midplane launcher toroidal steering angles ranging between 27 to 40 degrees to maximize the total driven current and the minor radial location off-axis. This resulted in the angles chosen to be 220 (lower), 218 (middle), and 218 (upper) for a deposition peak at $\rho \sim 0.35$, and ~ 700 kA for 20 MW. The LH spectra is peaked at $n_{\parallel} = 2.15$ and -3.9 , with $\Delta n_{\parallel} = 0.2$, and with 87% forward and 13% backward power weighting (which provides the factor of 1.6 enhancement over the reference weighting 72.5% forward and 27.5% backward).

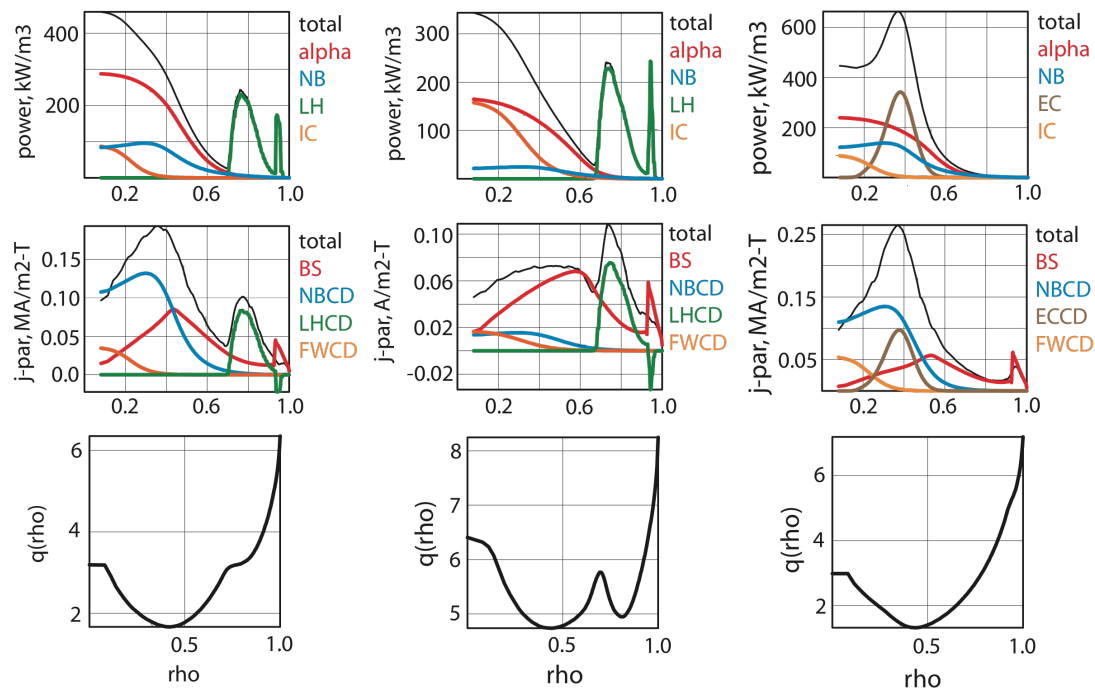


Figure 5. Profiles of the power deposition, parallel current density, and safety factor for $I_p = 10$ MA, $i_i(1) = 0.83$ NB/LH/IC, $I_p = 7.3$ MA, $i_i(1) = 0.54$ NB/LH/IC, and $I_p = 9.3$ MA, $i_i(1) = 1.15$ NB/EC/IC scenarios. In the first 2 cases 40 MW of LH is used, in the 3rd case 40 MW of EC is used.

Shown in Fig. 5 is parallel current density and safety factor profile from the combination of 24.5 MW of NB, 20 MW of IC, and 40 MW of LH, giving an $I_p = 10$ MA. This case has used the most peaked density profile, $n/n_{Gr} = 0.85$, $n(0)/\langle n \rangle = 1.5$, $\beta_N = 2.6$, $i_i(1) = 0.85$ and $i_i(3) = 0.69$, q_{\min} is 1.65, and $H_{98} = 1.60$. The current profile is dominated by the NB driven current since it is an efficient source and deposits close to the magnetic axis. In spite of the large LH power, which drives nearly 1.8 MA of current, it cannot effectively control the location of the minimum safety factor in

combination with high NB power. Fig. 5 shows a case with the NB power reduced to 8 MW, still with 40 MW of LH, where the safety factor is now increased to $q(0) = 6.3$ and $q_{\min} = 4.75$. The safety factor profile features are from the LH and the bootstrap current, and now the LH is competitive in shaping this profile. The medium density peaking is used here. Here $I_p = 7.3$ MA, $n/n_{Gr} = 1.0$, $n(0)/\langle n \rangle = 1.3$, $\beta_N = 2.4$, $li(1) = 0.54$ and $li(3) = 0.46$, and $H_{98} = 1.62$.

The use of 33 MW of NB, 20 MW of IC, and 20 and 40 MW of EC have been examined at a range of densities. The narrower deposition of the EC is peaked further out compared to the NB, but only a small amount, and so it largely adds to the broader NB current profile around $\rho = 0.35$. A 40 MW EC case is shown in Fig. 5, at $n/n_{Gr} = 0.83$, $n(0) = 0.75 \times 10^{20} / m^3$, $n(0)/\langle n \rangle = 1.5$, $I_p = 9.3$ MA, $li(1) = 1.15$, $li(3) = 0.92$, $\beta_N = 2.4$, $H_{98} = 1.55$. Fig. 5 shows the parallel current, power and safety factor profiles for this case. The contributions to the plasma current are $I_{BS} = 3.5$, $I_{NB} = 3.6$, $I_{EC} = 1.45$, and $I_{FW} = 0.4$ MA. The minimum safety factor is ~ 1.3 , and it maybe undesirable to have the 3/2 magnetic surface inside the plasma allowing a double tearing mode, however, stability analysis was not done. The minimum safety factor is higher for the 20 MW EC case, about 1.67.

TABLE I. Plasma parameters for steady state scenarios with 100% non-inductive plasma current

	NB+LH+IC	NB+LH+IC	NB+EC+IC	NB+EC+IC	NB+EC+LH
I_p , MA	10.0	7.25	7.75	9.25	9.25
I_{BS} , MA	4.6	4.85	3.33	3.54	4.12
I_{NB} , MA	3.1	0.55	3.27	3.6	3.83
I_{LH} , MA	1.77	1.85	0	0	0.94
I_{EC} , MA	0	0	0.7	1.46	0.6
I_{FW} , MA	0.25	0.25	0.25	0.4	0
P_{NB} , MW	24.5	8.0	33.0	33.0	33.0
P_{LH} , MW	40.0	40.0	0	0	20.0
P_{EC} , MW	0	0	20.0	40.0	20.0
P_{IC} , MW	20 \rightarrow 5	20	20 \rightarrow 5	20 \rightarrow 5	0
P_{α} , MW	74	43	40	55	60
P_{rad} , MW	38	27	26.5	32	29
Q	5.3	3.16	3.44	3.53	4.1
n/n_{Gr}	0.85	1.0	1.0	0.83	0.82
β_N	2.65	2.4	2.2	2.45	2.45
$li(1), li(3)$	0.85, 0.69	0.54, 0.46	1.07, 0.9	1.15, 0.92	0.85, 0.69
H_{98}	1.60	1.62	1.58	1.55	1.60
$q(0), q_{\min}$	2.9, 1.65	6.3, 4.75	2.0, 1.67	2.9, 1.3	3.6, 1.8
$n(0)/\langle n \rangle$	1.5	1.3	1.5	1.5	1.5
ρ_{ITB}, χ_{\min}	0.4	0.7	0.55	0.55	0.7

Table I shows various plasma parameters for the 3 cases described above, as well as for a 20 MW EC and a 20 MW EC/LH cases. Variations in the density from $n/n_{Gr} = 0.75$ to 1.0 indicate that the plasma current can be maintained within about 0.5-0.75 MA over this range as the bootstrap and driven currents compensate each other. Variations in the density peaking show that the lowest values give the lowest 100% non-inductive plasma currents, and visa versa, which is driven predominantly by the bootstrap current. The shape of the bootstrap current profile is mainly determined by the temperature gradient location. The fusion gains are in the range of 3-6, with

higher values reached with the higher densities, higher density peaking, and can be increased by accessing higher energy confinement or stepping down the IC power in flattop, which is only required to drive a small amount of current on axis.

5. Conclusions

The advanced operating scenarios in ITER are important to explore the configurations that can become the basis for fusion power plants. The simulation studies have found that the hybrid scenario at 12.5 MA can access 900-1300 s flattop burn times and remain within the CS and PF coil limits. The operating space for this scenario is large and can support a wide range of plasma and discharge conditions. The non-inductive current fraction is about 0.35, $\beta_N \sim 2-2.2$, and $H_{98} \sim 1.25$, yielding $Q \sim 7$. Further work will examine higher and lower plasma currents, and impact of higher beta via improved confinement or a higher pedestal.

The simulation studies of the steady state scenario have found that the range of plasma currents, $I_p = 7.3-10$ MA, can remain within CS and PF coil limits, in particular, because the flattop phase stops consuming V-s. To obtain 100% non-inductive plasma current and $Q \sim 3-6$ with EPED predictions for the pedestal pressure height, improved core confinement over H-mode is required. A target of $H_{98} \sim 1.6$ yields a wide range of plasma currents depending on sources used and density peaking. The resulting β_N values are about 2.3-2.5, $li(3)$ values are 0.46-1.15, and n/n_{Gr} are 0.75-1.0. Further work will examine additional source combinations, larger inboard wall gaps, and H to L transitions.

This work was supported by the US Department of Energy under DE-AC02-CH0911466. The views and opinions expressed herein do not necessarily reflect those of the ITER Organization

References

- [1] ITER Physics Basis, Nuc Fus **39** 1999; Progress in ITER Physics Basis, Nuc Fus **47** 2007.
- [2] JARDIN, S.C., et al., 1986 J. Comput. Phys. **66** 481.
- [3] KRITZ, A.H., et al., this conference.
- [4] STAEBLER G M *et al* 1997 *Nucl. Fusion* **37** 287; J. E. KINSEY et al 2005 **12** 052503-1.
- [5] HALPERN, F. *et al.*, Phys. Plasmas **15**, 012304 (2008); WEILAND, J. *et al.*, Nucl. Fusion **49**, 965933 (2009).
- [6] SNYDER, P. et al 2009 Nuc Fus **49** 085035.
- [7] KIKUSHKIN, A. S. et al 2007 Nuc Fus **47** 698.
- [8] M. BRAMBILLA 1996 A Full Wave Code for Ion Cyclotron Waves in Toroidal Plasmas, Rep. IPP 5/66, Max-Planck-Institut für Plasmaphysik, Garching.
- [9] R. J. GOLDSTON et al 1981 J. Comput. Phys. **43** 61.
- [10] A. H. KRITZ et al 1982 Heating in Toroidal Plasmas, Proc. 3rd Joint Varenna-Grenoble Int. Symp. Grenoble, 1982, Vol. 2 CEC, Brussels (1982) 707.
- [11] D. W. IGNAT et al 1994 Nucl. Fusion **34** 837.
- [12] HARVEY, R. W. and McCOY, M. G., Proceedings of the IAEA Technical Committee on Advances in Simulation and Modeling of Thermonuclear Plasmas, Montreal, Quebec (International Atomic Energy Agency, Vienna, 1993), p. 489.
- [13] KESSEL, C.E., et al. Nuc Fus 2009.
- [14] KESSEL, C.E., et al. Nuc Fus 2007.